Published in final edited form as:
Urology. 2010 April ; 75(4): 914–922. doi:10.1016/j.urology.2009.10.031.

2,8-Dihydroxyadenine nephrolithiasis Induces Developmental Stage-specific Alterations in Gene Expression in Mouse Kidney

Jianmin Chen[1], **Yanping Chen**[1], **Stephanie Capizzi**[1,2], **Min Yang**[1], **Li Deng**[1], **Sharon B. Bledsoe**[3], **Andrew P. Evan**[3], **Jay A. Tischfield**[1], and **Amrik Sahota**[1]

[1]Department of Genetics, Rutgers University, Piscataway, New Jersey, USA

[3]Department of Anatomy and Cell Biology, Indiana University School of Medicine, Indianapolis, Indiana, USA

Abstract

Objectives—Kidney stone diseases are common in premature infants, but the underlying molecular and cellular mechanisms are not fully defined. We carried out a prospective observational study using microarray analysis to identify factors that may be crucial for the initiation and progression of stone-induced injury in the developing mouse kidney.

Methods—Mice with adenine phosphoribosyltransferase (APRT) deficiency develop 2,8-dihydroxyadenine (DHA) nephrolithiasis. Gene expression changes between *Aprt*$^{-/-}$ and *Aprt*$^{+/+}$ kidneys from newborn and adult mice were compared using Affymetrix gene chips. Targets of interest were further analyzed by quantitative real time PCR and immunohistochemistry.

Results—We identified a set of genes that were differentially expressed in the developing kidney in response to DHA-induced injury. In 1-week-old *Aprt*$^{-/-}$ mice, the expression of *Sprr2f* and *Clu* was highly augmented and that of *Egf* was significantly decreased. We also observed that maturation-related gene expression changes were delayed in developing *Aprt*$^{-/-}$ kidneys and immature *Aprt*$^{-/-}$ kidneys contained large numbers of intercalated cells blocked from terminal differentiation.

Conclusions—This study presents a comprehensive picture of the transcriptional changes induced by DHA stone injury in the developing mouse kidney. Our findings help explain growth impairment in kidneys subject to injury during the early stages of development.

Keywords

Adenine phosphoribosyltransferase deficiency; 2,8-dihydroxyadenine nephrolithiasis; developing kidney; crystal-induced cell injury; microarray analysis

Correspondence: Amrik Sahota, Department of Genetics, Life Sciences Building, Rutgers University, 145 Bevier Road, Piscataway, NJ 08854, USA, Phone: 732-445-7185 Fax: 732-445-1147 sahota@biology.rutgers.edu.
[2]Present address: Department of Pathology and Laboratory Medicine, Robert Wood Johnson Medical School, University of Medicine and Dentistry of New Jersey, Piscataway, New Jersey

Introduction

Kidney stones are common in premature infants and in renal transplant patients. Proliferating renal tubular cells in developing or regenerating kidneys likely account for this high incidence[1]. Indeed, crystals are known to bind rapidly to the surface of proliferating, but not quiescent renal epithelial cells[2,3]. Therefore, the target cells of initial crystal-induced injury likely are immature renal tubular cells. However, our current understanding of stone disease is based largely on data obtained from biopsies taken at advanced stages of disease progression; confluent monolayer cells treated with calcium oxalate crystals; or adult rats fed with ethylene glycol, which is nephrotoxic. These may not be the most suitable models for studying the molecular and cellular pathways involved in the initial renal response to crystal injury.

2,8-Dihydroxyadenine (DHA) nephrolithiasis due to adenine phosphoribosyltransferase (APRT) deficiency is a rare metabolic disorder, but it shares important characteristics, such as intratubular crystal retention, inflammation, and fibrosis with stone diseases caused by other metabolic disorders[4] or induced by surgical procedures such as intestinal bypass surgery[5]. Patients with brushite stones also form intratubular crystals accompanied by extensive inflammation and fibrosis[6]. APRT-deficient mice develop DHA nephrolithiasis, in much the same way as humans do[7-9]. The two major pathological outcomes in these mice are renal fibrosis and kidney growth retardation[7-10]. DHA crystal deposition in the kidney starts while the kidney is still developing, and gradually affects all segments, from tubular epithelia to interstitial cells, so it appears to be an appropriate model for studying temporal and spatial (renal segment or cell type specific) responses to crystal-induced injury.

Nephrogenesis in humans is complete within 34-36 weeks of gestation. In contrast, formation of new nephrons in mice continues for up to two weeks following birth[11]. Therefore kidneys from 1-week-old mice may be a useful model for studying the early stages of development and their response to injury. Given that growth retardation is characteristic of kidneys subjected to injury during early development and interstitial fibrosis is the major pathological result in injured adult kidneys, we hypothesized that DHA crystal injury induces distinct gene expression alterations in kidneys from 1-week-old pups and that these early response genes might be important in directing the final outcome of DHA injury, including growth retardation. To test this hypothesis, we carried out gene expression profiling in 1-week-old (developing) and 1-month-old (developed) *Aprt*$^{-/-}$ and wild type mouse kidneys.

Material and Methods

Specimens

Aprt$^{+/-}$ mice of strain 129 were mated and the *Aprt* genotype and gender of the progeny determined by multiplex PCR of tail DNA. Pathological changes were not seen in kidneys from wild-type or heterozygous mice, but a small number of heterozygotes had some crystals in the kidney[10]. Kidneys were dissected from wild type and *Aprt*$^{-/-}$ mice. One kidney was immersed in RNAlater™ (Qiagen, Valancia, CA) and stored at -80°C prior to RNA or protein extraction. The other kidney was fixed in 4% paraformaldehyde prior to processing for paraffin sectioning.

DNA Microarray

For microarray comparison, littermate pairs (*Aprt*$^{-/-}$ and *Aprt*$^{+/+}$) of the same sex were selected to minimize variability. Six pairs (three male and three female) were aged one week and three pairs (two male and one female) were aged one month.. RNA was hybridized to Affymetrix (Santa Clara, CA) GeneChip MG-U74Av.2 arrays following standard protocol.

Briefly, total RNA was purified from whole kidney and double stranded cDNA was synthesized using T7-$[dT]_{24}$ primer and the SuperScript Double-Stranded cDNA Synthesis Kit (Invitrogen, Carlsbad, CA). Biotin-labeled cRNA was generated by *in vitro* transcription using a BioArray High Yield RNA Transcript Labeling Kit (Enzo Diagnostics, Farmingdale, NY). cRNA was hybridized to the arrays at 45°C for about 18 hour. Arrays were washed, stained, and scanned using a GeneChip Fluidics Station 450 and a GeneArray Scanner. The dataset has been uploaded to the NCBI Gene Expression Omnibus database (GEO, accession # GSE18160.

Data Analysis

Microarray data were analyzed two ways to identify differentially expressed genes. First, gene expression levels were assessed using GeneChip® Operating Software (GCOS 1.0, Affymetrix) with default statistical settings. Each array was scaled to a target signal of 500/probe set and the normalization factor was 1.0. Paired comparisons were made using the Affymetrix standard algorithm. Replicate sets collected and hybridized on different days were analyzed separately and the data then pooled. Genes showing consistent increase or decrease across all replicate sets were considered to be differentially expressed. Second, Affymetrix image files were imported into GeneSpring 7.0 (Silicon Genetics, Redwood City, CA) and processed using the GeneChip Robust Multiarray Averaging (GC-RMA) procedure. Normalized data that passed the one-sided student t-test ($p \leq 0.05$) were then subjected to further statistical analyses (Welch t-test, $p < 0.05$) to identify genes differentially expressed in different *Aprt* genotypes or age groups. In brief, genes were first ranked by statistical significance and then corrected for multiple comparisons. Only those genes with a false discovery rate (FDR) of $q \leq 0.05$ were retained as early response genes.

Functional Analysis

Hierarchical clustering—To identify the expression pattern of the early response genes during kidney development, hierarchical clustering was performed using the “Clustering \Gene Tree” function in GeneSpring with default settings.

EASE—To further characterize biologically relevant pathways, lists of differentially expressed genes induced by DHA in immature or mature kidneys were analyzed using the categorical over-representation function of Expression Analysis Systematic Explorer (EASE) from the National Institute for Allergy and Infectious Diseases[12]. The most significantly over-represented categories/pathways were identified using EASE scores.

GSEA—Gene Set Enrichment Analysis (GSEA) was carried out as described[13] using GSEA v.2. Probe sets were collapsed to gene symbol, then genes were ranked using $Aprt^{-/-}$ to $Aprt^{+/+}$ ratios. The cumulative distribution function was constructed by performing 1,000 random sample assignments; thus, the smallest obtainable p value was 1×10^{-3}.

Real time PCR

Total RNA was reverse transcribed using the TaqMan Reverse Transcription Reagent Kit (Applied Biosystems, Foster City, CA). Targets were amplified by real time PCR using the GeneAmp 7900 Sequence Detection System and Sybr Green Master Mix (Applied Biosystems) for 40 cycles. Kidneys from six or more mice were used for each age or genotype group and all experiments were carried out in triplicate. Arbitrary mRNA level for each test sample was calculated using a standard dilution curve. Hprt or Gapdh expression was used as internal control to normalize the expression levels of genes of interest.

Immunohistochemistry and Immunofluorescence

Immunohistochemistry—Paraffin sections were treated with boiling citrate buffer (0.01 M, pH 6) to unmask antigens. Endogenous peroxidase activity was blocked with 0.3% H_2O_2 in methanol. Sections were first incubated in blocking solution (Vectastain Elite ABC Kit, Vector Laboratories, Burlingame, CA), then in anti-small proline-rich protein 2 (Sprr2) antibody (1:1,000 dilution, Apotech, Zurich, Switzerland) overnight at 4°C in a humidified chamber. The following day, sections were incubated in biotinylated secondary antibody, in ABC reagent (Vector Laboratories), and then in peroxidase substrate solution (3,3′-diaminobenzidine). The slides were counterstained with hematoxylin, dehydrated, cleared in xylene, and mounted in VectorMount (Vector Laboratories). Proliferating cell nuclear antigen (PCNA) staining was carried out following the protocol provided with the PCNA Staining Kit (Zymed Laboratories Inc., South San Francisco, CA).

Immunofluorescence—Paraffin sections were blocked in 1% BSA in PBS, then incubated at 4°C overnight in the primary antibody mixture of anti-Sprr2 and anti-stage-specific embryonic antigen 1 (Ssea-1) (Santa Cruz Biotechnology, Santa Cruz, CA) diluted to 1:500 and 1:200, respectively. Secondary antibodies Alexa Fluor®488 goat anti-rabbit IgG and Alexa Fluor®594 goat anti-mouse IgG (Invitrogen, Carlsbad, CA) were diluted 1:400. Sections were counterstained with DAPI and mounted using the SlowFade® Antifade Kit (Invitrogen).

Results

Gene Expression Changes Induced by DHA are Developmental Stage-specific

To examine gene expression changes with respect to kidney developmental stage, six sets of 1-week-old *Aprt*$^{-/-}$ and *Aprt*$^{+/+}$ littermate pairs were analyzed using the pair comparison function in GCOS 1.0. One hundred and twenty and 74 genes were identified as differentially expressed in male and female *Aprt*$^{-/-}$ mice, respectively (Figure 1). We also examined three sets of 1-month-old littermate pairs. Sixty-six and 50 genes were differentially expressed in males and females of this age group, respectively. There were only 15 and 7 genes that were in common in males and females, respectively, in the two age groups. This is less than 15% of the 120 or 74 genes found in kidneys from 1-week-old male or female mice (Figure 1). These data demonstrate that DHA-induced gene expression changes in APRT-deficient mice are developmental stage-specific.

Next we used EASE to identify biological schemes within lists of differentially expressed genes (Table 1). The list of genes induced by DHA in 1-week-old kidneys was highly enriched with genes important for response to external stimuli, whereas the list of genes from 1-month-old mice was significantly enriched with genes for lipid metabolism. The biological processes with the lowest EASE scores were defense response ($p \leq 0.0000005$) for 1-week-old mice and steroid metabolism ($p \leq 0.00002$) for 1-month-old mice.

EASE focuses on lists of differentially expressed genes, leaving out the contributions of genes with small expression level changes. To fully utilize the microarray data, we also examined age differences by comparing the top 100 gene sets enriched in 1-week-old with those in 1-month-old kidneys using GSEA. The gene overlap between 1-week-and 1-month-old kidneys was low (19%), and included genes up-regulated during epithelial-mesenchymal transition and in aging human kidneys. Gene sets showing age-specific enrichment only in 1-week-old APRT-deficient mice included interleukin 6 (*Il6*) target genes and genes down-regulated in stem cells. Transforming growth factor beta (*Tgfβ*) target genes and genes induced during inflammatory response were preferentially induced in kidneys from 1-month-old APRT-deficient mice.

To validate microarray data, real time PCR was carried out on a group of 20 genes, including *Sprr2f*, *Clu*, *Lcn2*, and *Egf*. The real time results correlated well with the microarray data. Figure 1 (lower panel) shows the real time PCR results for *Sprr2f*, clusterin (*Clu*), and epidermal growth factor (*Egf*). Expression of *Sprr2f* and *Clu* was highly augmented in 1-week-old *Aprt*$^{-/-}$ mice; in contrast, *Egf* mRNA levels decreased significantly in *Aprt*$^{-/-}$ pups. The expression patterns of these three genes in kidneys from mice at age 1-, 3, and 6-months were markedly different from those from 1-week-old *Aprt*$^{-/-}$ mice. These data provide further support for our observation that immature kidneys respond to DHA differently compared with mature kidneys.

DHA Injury Delays Kidney Maturation

To identify early response genes, we combined the two lists of differentially expressed genes generated by GCOS pair comparison and group comparison (FDR, $q \leq 0.05$) using the Affymetrix CDF data file format. A total of 68 genes identified by both methods were selected as early response genes (Table 2). Among these are genes known to be involved in kidney stone injury, including matrix gla protein (*Mgp*) and monocyte chemoattractant protein 1 (*Mcp1*); genes known to be involved in injury-induced cell cycle arrest, including 14-3-3-sigma and growth arrest DNA-damage-inducible beta (*Gadd45b*); a broad list of genes known to be involved in kidney development, including *Sprr2f*, cytokeratin 19 (*Ckt 19*), lipocalin 2 (*Lcn2*), and *Clu*; genes that are important for kidney maturation, including *Egf*; and genes involved in inflammatory response, including interleukin 1b (*Il1b*).

The early response genes were profiled on the basis of similarity of their temporal expression patterns, using hierarchical cluster analysis in GeneSpring 7.0. There was a clear inverse correlation between DHA-induced and maturation-related gene expression changes. Most genes down-regulated in *Aprt*$^{-/-}$ pups had higher expression in mature kidneys. Conversely, 20 out of the 61 genes up-regulated in *Aprt*$^{-/-}$ pups had lower expression in mature kidneys (Figure 2). These observations suggest that DHA injury delays maturation-related gene expression changes. In other words, 1-week-old *Aprt*$^{-/-}$ kidneys are less mature than *Aprt*$^{+/+}$ kidneys of the same age.

We noted a high degree of overlap between the expression of up-regulated early response genes in the present study and in a study of leukemia inhibitory factor (LIF)-sustained pluripotency markers in stem cells[14]. Of the 41 LIF-sustained-pluripotency markers, 14 overlapped with DHA-induced early response genes, including *Socs3*, *Osmr*, *Ccl2*, *Vcam1*, *Fos*, and *Egr1*. To substantiate this observation, GSEA was performed against this set of genes. LIF-sustained pluripotency markers were found to be significantly enriched in genes up-regulated in immature *Aprt*$^{-/-}$ kidneys ($p = 0.007$)

(Figure 3). In addition, GSEA analysis using the Molecular Signatures database (MSigDB) selected previously identified LIF target genes as well[15]. LIF signaling pathways play a critical role in the maturation of kidneys[16]. Therefore, it is likely that delayed maturation in APRT-deficient kidneys is mediated through the LIF pathway.

Collecting Ducts in Immature *Aprt*$^{-/-}$ Kidneys Consist Mainly of Intercalated Cells Expressing Sprr2 and Ssea-1

Sprr2f is a gene of considerable interest because of its potential role in tissue regeneration. High *Sprr2f* expression was detected during normal nephrogenesis around embryonic day 16.5 (E16.5)[17]. By immunohistochemistry, very few Sprr2 immnuo-positive cells could be detected in immature wild type kidneys (Figure 4A). In contrast, extensive Sprr2 staining was seen in the collecting tubules *of Aprt*$^{-/-}$ pups (Figure 4B), and there was dilation and hyperplasia of collecting ducts in kidneys from these pups. To clarify whether these changes

were the result of cellular proliferation, we stained sections with anti-PCNA antibody. In adult kidney, tubular cell injury and regeneration occurs concurrently[18]. Unexpectedly, the enlarged collecting tubules from kidneys from *Aprt*$^{-/-}$ pups were largely PCNA immuno-negative (Figure 4C, D). These cells did not appear to be apoptotic by their nuclear morphology, which was confirmed by TUNEL assay and caspase 3 staining (data not shown).

Cell morphology suggests that Sprr2 immuno-positive cells are intercalated cells, not principal cells. *In vitro*, β intercalated cells can give rise to principal cells, but not the other way around[19]. Thus, Sprr2 immuno-positive cells may be early lineage cells blocked from further differentiation in response to DHA injury. We stained kidney sections for Ssea-1, a widely used mouse stem cell pluripotency marker. Ssea-1 immuno-positive cells are found at the tips of branching ureteric buds during nephrogenesis, which disappear after fusing with the S structure[20]. Sprr2 immuno-positive cells were all Ssea-1 positive, suggesting that DHA injury blocks further differentiation of the immature collecting duct cells.

Comment

In mice, 90% of nephrogenesis occurs in the first two weeks after birth, so neonatal *Aprt*$^{-/-}$ mice provide a unique opportunity to study the response of immature nephrons to crystal-induced injury. In the current study, we examined genes or pathways induced in kidneys from immature and mature *Aprt*$^{-/-}$ mice in response to DHA crystals. Noticeably, many more genes were induced in immature kidneys than in mature kidneys (Figure 1). In other words, many of the early responses, including Sprr2f expression, are temporal and unique to the developing kidney.

Sprr2f mRNA and protein is highly elevated in *Aprt*$^{-/-}$ pups and induction disappears completely in 1-month-old mice. Small proline-rich proteins are precursors of the cornified envelope of squamous epithelia. *Sprr2f* is briefly expressed at late stages of nephrogenesis[17], and has the unique characteristic of being highly expressed in the uterus and ovary[21,22]. The physiological role of *Sprr2f* in these organs is still unclear, but there have been several reports on other members of the Sprr family, mainly *Sprr1a* and *2a*, promoting post injury regeneration. *Sprr1a* is induced immediately after axon injury and the over-expression of *Sprr1a* promoted neuron regeneration by modulating actin-based motility[23]. *Sprr1a* is reported to act as a stress-inducible cardio-protective protein[24]. Higher levels of *Sprr2a* message correlated with better adaptation in small bowl resection[25]. Deficiency in Sprr2 expression in biliary epithelial cells from *Il6*$^{-/-}$ mice after bile duct ligation was associated with impaired barrier function[26]. These observations suggest that *Sprr2f* may have protective effects in stone injury.

By immunohistochemistry, Sprr2 protein was localized strictly in the collecting ducts in 1-week-old *Aprt*$^{-/-}$ mice that are Ssea-1 immuno-positive (Figure 4). Co-localization of Sprr2 and Ssea-1 in collecting duct cells suggests that DHA injury possibly delays the maturation process of collecting ducts. Consistent with this notion, Clu, a marker for immaturity of collecting duct cells[27], was up-regulated in *Aprt*$^{-/-}$ pups. Clu is first detected in the condensing nephrogenic mesenchyme and is subsequently down-regulated during maturation. Egf treatment can reduce Clu levels in cystic kidneys and rescue some aspects of the phenotype[28]. Reduced expression of Egf in *Aprt*$^{-/-}$ mice also supports the concept of delayed maturation in collecting ducts. Taken together, these findings link *Sprr2f* to collecting duct development. However, cells with elevated levels of *Sprr2f* are not proliferating renal progenitors, because Sprr2 immunoreactivity inversely correlates with PCNA staining (Figure 4C-4D). Therefore, over-expression of *Sprr2f* may represent a transition state between renal progenitors and mature collecting duct cells. These cells likely

further differentiate into mature epithelial cells under normal developmental conditions. We did not detect co-localization of Sprr2 expression with the presence of DHA crystals in collecting ducts, most likely due to the loss of crystalline material during tissue preparation[8,10].

Given that induction of *Sprr2f* is specific to immature APRT-deficient kidneys, while up-regulation of *Sprr1a* and *Sprr2a* is seen in both immature and mature kidneys, which are regulated by Il6 signaling, we hypothesize that Sprr2f expression may be regulated through LIF/Stat3, which plays an essential role in nephrogenesis. In the presence of LIF signaling, mesenchymal cells expand and then convert into epithelia and form nephrons; in the absence of LIF signaling, these cells become apoptotic[16]. Interestingly, high levels of LIF strongly block mesenchymal cell induction, leading to a large number of stable epithelialized aggregates that do not develop further. This effect is reported to be reversible[29], suggesting a possible defense mechanism for immature cells in response to temporary stress. In APRT deficiency, DHA injury is chronic, so this block of further differentiation continues, leading to kidney growth retardation.

Conclusions

Two major conclusions can be drawn from the studies presented here. First, they help explain reduced fibrosis and growth impairment in kidneys subject to injury during the early stages of development, thus providing potential targets for manipulating these two crucial processes in kidney stone disease. Second, gene expression is cell-type specific and we recognize the limitations of studying these changes in whole kidney tissue. The physiological significance of many of the newly identified genes in renal injury remains to be demonstrated, thus providing valuable leads for future direction.

Acknowledgments

We thank Drs. Changshun Shao, Li Liang, and Hristo Houbaviy for suggestions and comments. Dr. David Denhardt provided valuable technical advice; Dr. David Axelrod assisted with image analysis software; and Dr. Kenneth Ruehl assisted with Sprr2 immunohistochemistry.

References

1. Verhulst A, Asselman M, De Naeyer S, et al. Preconditioning of the distal tubular epithelium of the human kidney precedes nephrocalcinosis. Kidney Int. 2005; 68:1643–1647. [PubMed: 16164641]
2. Verkoelen CF, van der Boom BG, Houtsmuller AB, et al. Increased calcium oxalate monohydrate crystal binding to injured renal tubular epithelial cells in culture. Am J Physiol. 1998; 274:F958–965. [PubMed: 9612335]
3. Asselman M, Verhulst A, Van Ballegooijen ES, et al. Hyaluronan is apically secreted and expressed by proliferating or regenerating renal tubular cells. Kidney Int. 2005; 68:71–83. [PubMed: 15954897]
4. Sahota, AS.; Tischfield, JA.; Kamatani, N.; Simmonds, HA. Adenine phosphoribosyltransferase deficiency and 2,8-dihydroxyadenine lithiasis. In: Scriver, CR., editor. The Metabolic and Molecular Bases of Inherited Disease. 8th. New York: McGraw-Hill; 2001. p. 2571-2584.
5. Evan AP, Lingeman JE, Coe FL, et al. Randall's plaque of patients with nephrolithiasis begins in basement membranes of thin loops of Henle. J Clin Invest. 2003; 111:607–616. [PubMed: 12618515]
6. Evan AP, Lingeman JE, Coe FL, et al. Crystal-associated nephropathy in patients with brushite nephrolithiasis. Kidney Int. 2005; 67:576–591. [PubMed: 15673305]
7. Engle SJ, Stockelman MG, Chen J, et al. Adenine phosphoribosyltransferase-deficient mice develop 2,8-dihydroxyadenine nephrolithiasis. Proc Natl Acad Sci USA. 1996; 93:5307–5312. [PubMed: 8643571]

8. Redhead NJ, Selfridge J, Wu CL, Melton DW. Mice with adenine phosphoribosyltransferase deficiency develop fatal 2,8-dihydroxyadenine lithiasis. Hum Gene Ther. 1996; 7:1491–1502. [PubMed: 8864750]
9. Stockelman MG, Lorenz JN, Smith FN, et al. Chronic renal failure in a mouse model of human adenine phosphoribosyltransferase deficiency. Am J Physiol. 1998; 275:F154–F163. [PubMed: 9689017]
10. Evan AP, Bledsoe SB, Connors BA, et al. Sequential analysis of kidney stone formation in the Aprt knockout mouse. Kidney Int. 2001; 60:910–923. [PubMed: 11532086]
11. Frith, CH.; Terracini, B.; Turusov, VS. Tumours of the kidney, renal pelvis and ureter. In: Turusov, VS., editor. Pathology of Tumours in Laboratory Animals. 2nd. Vol. Vol II -Tumours of the Mouse. Lyon: IARC Scientific Publication No. 111; 1994. p. 357-381.
12. Hosack DA, Dennis G Jr, Sherman BT, et al. Identifying biological themes within lists of genes with EASE. Genome Biol. 2003; 4:R70. [PubMed: 14519205]
13. Subramanian A, Tamayo P, Mootha VK, et al. Gene set enrichment analysis: a knowledge-based approach for interpreting genome-wide expression profiles. Proc Natl Acad Sci USA. 2005; 102:15545–15550. [PubMed: 16199517]
14. Palmqvist L, Glover CH, Hsu L, et al. Correlation of murine embryonic stem cell gene expression profiles with functional measures of pluripotency. Stem Cells. 2005; 23:663–680. [PubMed: 15849174]
15. Abbud RA, Kelleher R, Melmed S. Cell-specific pituitary gene expression profiles after treatment with leukemia inhibitory factor reveal novel modulators for proopiomelanocortin expression. Endocrinology. 2004; 145:867–880. [PubMed: 14576184]
16. Barasch J, Yang J, Ware CB, et al. Mesenchymal to epithelial conversion in rat metanephros is induced by LIF. Cell. 1999; 99:377–386. [PubMed: 10571180]
17. Schwab K, Patterson LT, Aronow BJ, et al. A catalogue of gene expression in the developing kidney. Kidney Int. 2003; 64:1588–1604. [PubMed: 14531791]
18. Nouwen EJ, Verstrepen WA, Buyssens N, et al. Hyperplasia, hypertrophy, and phenotypic alterations in the distal nephron after acute proximal tubular injury in the rat. Lab Invest. 1994; 70:479–493. [PubMed: 7909858]
19. Fejes-Toth G, Naray-Fejes-Toth A. Differentiation of renal beta-intercalated cells to alpha-intercalated and principal cells in culture. Proc Natl Acad Sci USA. 1992; 89:5487–5491. [PubMed: 1608958]
20. Fleming S. N-linked oligosaccharides during human renal organogenesis. J Anat. 1990; 170:151–160. [PubMed: 1701421]
21. Song HJ, Poy G, Darwiche N, et al. Mouse Sprr2 genes: a clustered family of genes showing differential expression in epithelial tissues. Genomics. 1999; 55:28–42. [PubMed: 9888996]
22. Cabral A, Voskamp P, Cleton-Jansen AM, et al. Structural organization and regulation of the small proline-rich family of cornified envelope precursors suggest a role in adaptive barrier function. J Biol Chem. 2001; 276:19231–19237. [PubMed: 11279051]
23. Bonilla IE, Tanabe K, Strittmatter SM. Small proline-rich repeat protein 1A is expressed by axotomized neurons and promotes axonal outgrowth. J Neurosci. 2002; 22:1303–1315. [PubMed: 11850458]
24. Pradervand S, Yasukawa H, Muller OG, et al. Small proline-rich protein 1A is a gp130 pathway- and stress-inducible cardioprotective protein. EMBO J. 2004; 23:4517–4525. [PubMed: 15510217]
25. Stern LE, Erwin CR, Falcone RA, et al. cDNA microarray analysis of adapting bowel after intestinal resection. J Pediatr Surg. 2001; 36:190–195. [PubMed: 11150463]
26. Nozaki I, Lunz JG III, Specht S, et al. Small proline-rich proteins 2 are noncoordinately upregulated by IL-6/STAT3 signaling after bile duct ligation. Lab Invest. 2005; 85:109–123. [PubMed: 15558059]
27. Harding MA, Chadwick LJ, Gattone VH, Calvet JP. The SGP-2 gene is developmentally regulated in the mouse kidney and abnormally expressed in collecting duct cysts in polycystic kidney disease. Dev Biol. 1991; 146:483–490. [PubMed: 1864465]

28. Gattone VH, Lowden DA, Cowley BD Jr. Epidermal growth factor ameliorates autosomal recessive polycystic kidney disease in mice. Dev Biol. 1995; 169:504–510. [PubMed: 7781894]

29. Bard JB, Ross AS. LIF, the ES-cell inhibition factor, reversibly blocks nephrogenesis in cultured mouse kidney rudiments. Development. 1991; 113:193–198. [PubMed: 1764994]

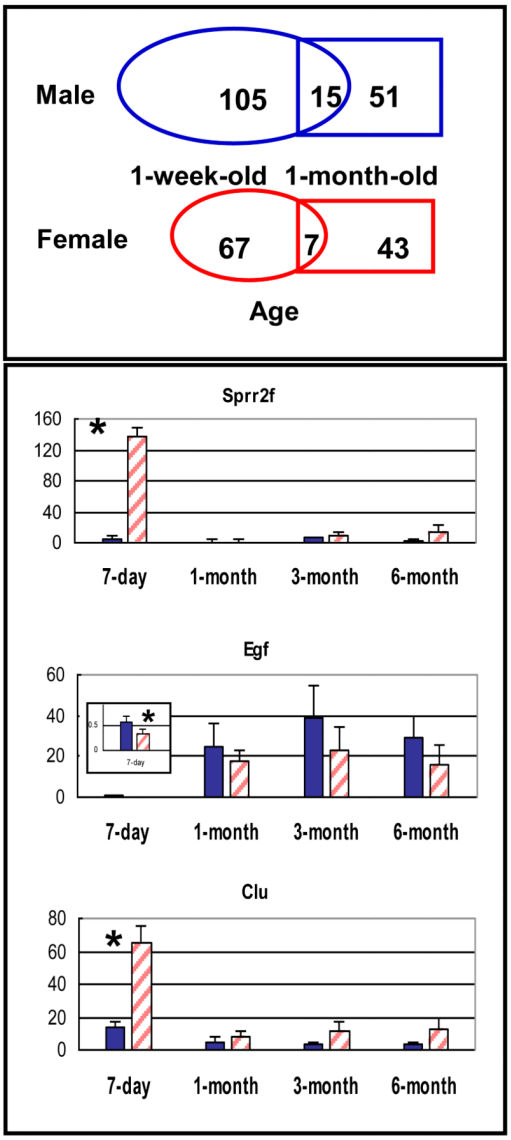

Figure 1. Pairwise overlap test and age-specific gene expression

Upper panel: Venn diagrams of pairwise overlap test. Numbers represent total number of genes differentially expressed in a specific age group or gender comparing *Aprt*$^{-/-}$ and wild type mice. Oval, 1-week-old; rectangle, 1-month-old. Blue, male; red, female. Lower panel: Age-specific gene expression. mRNA levels were measured by real-time PCR and normalized to *Hprt* expression. Bar color: blue (*Aprt*$^{+/+}$), pink (*Aprt*$^{-/-}$) Y-axis, the ratio between gene of interest and the internal control gene (*Hprt*). Insert is the zoomed-in image of 1-week-old kidneys which have very low *Egf* expression. * indicates $p<0.05$ (Welch's t-test).

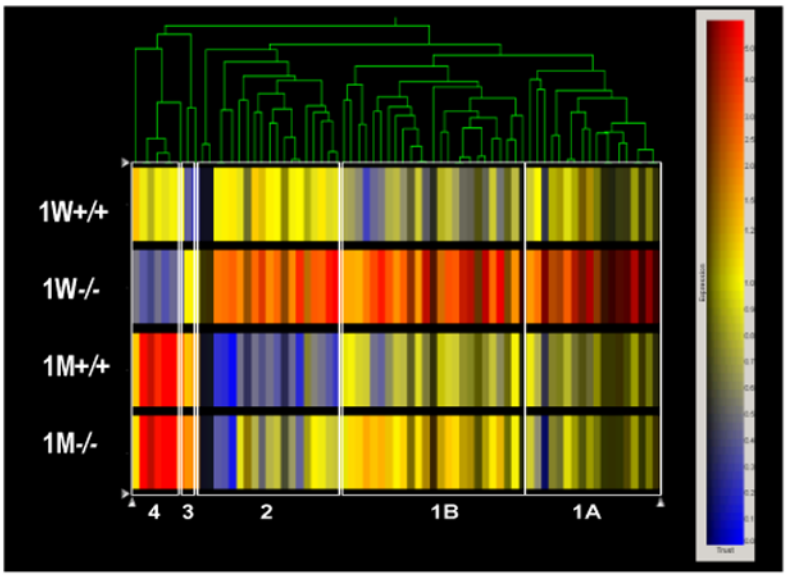

Figure 2. Heatmap of hierarchical clustering of early response genes

The diagram shows reverse expression patterns of maturation-related and DHA injury-related genes. Sixty eight early response genes were clustered according to their temporal expression pattern using GeneSpring. Each vertical bar represents a gene and its average mRNA level in each age/genotype group (1W = 1-week-old; 1M = 1-month-old). Expression level color scheme is shown on the right: red >blue, dark red, high mRNA level; dark blue, no expression. Four 1st degree clusters were found. Clusters 1-3 represent genes with augmented expression in 1-week-old *Aprt*$^{-/-}$ mice whereas cluster 4 shows genes with reduced expression in these mice. Expression levels of these genes remain mostly unchanged when comparing 1-month-old *Aprt*$^{-/-}$ mice with age-matched controls, suggesting that the expression changes are unique to immature kidneys. Importantly, all genes in clusters 2 and 4 show reverse expression patterns when comparing 1-week-old to 1-month-old controls (kidney maturation) and 1-week-old *Aprt*$^{-/-}$ to 1-week-old controls (kidney injury), suggesting that injury delays maturation in developing kidneys.

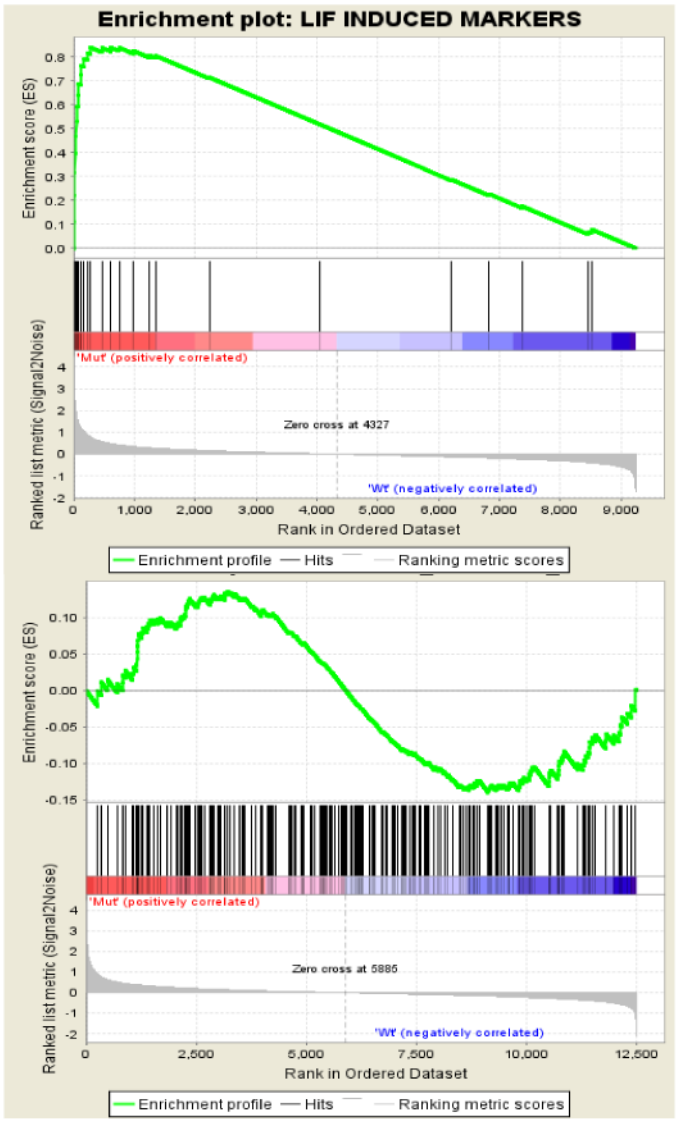

Figure 3. LIF-sustained pluripotency markers

LIF-sustained pluripotency markers were significantly enriched among genes up-regulated in immature APRT-deficient kidneys. There were 9,239 genes after collapsing the 12,488 native probes present on the microarray. Upper panel: From left to right, the lines indicate the relative positions of the 9,239 genes within the rank order from the probe most up-regulated in *Aprt*$^{-/-}$ kidneys to the probe most down-regulated (*Aprt*$^{-/-}$ to *Aprt*$^{+/+}$ log2 ratio from 4.4 to –1.7). The genes near the middle are unaffected by APRT deficiency, with *Aprt*$^{-/-}$ vs. *Aprt*$^{+/+}$, log2 ratio equals 1. Lower panel: An example of indiscriminate distribution of a gene set with no bias toward *Aprt*$^{-/-}$ or *Aprt*$^{+/+}$. In the upper panel, the LIF target genes are clearly enriched among genes up-regulated in immature *Aprt*$^{-/-}$ kidneys as evidenced by the increased density of black lines on the left side of the distribution, the positive enrichment score, and a nominal p = 0.007.

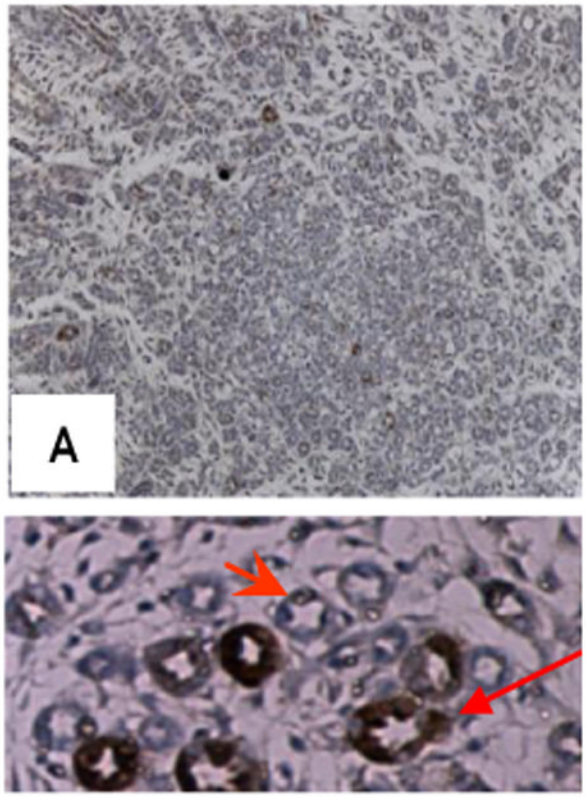

Figure 4. Sprr2, PCNA, and Ssea-1 immunostaining

Strong Sprr2 staining is detected only in collecting duct cells in immature APRT-deficient kidneys (B), but not in age-matched wild type kidneys (A). Sprr2 immuno-positive collecting duct cells (C, large arrow) in the developing mouse kidney are PCNA immuno-negative (D, large arrow), whereas Sprr2 immuno-negative cells are PCNA immuno-positive (C and D, small arrows). Sprr2 immuno-positive cells (green) are also Ssea-1 immuno-positive (red) (E). (F) is same as (E), but with higher magnification.

Table 1

List of gene categories over-represented in kidneys from 1-week- or 1-month-old APRT-deficient mice.

Gene Category	EASE score
1-week-old	
defense response	4.80E-07
Immune response	6.90E-07
response to biotic stimulus	1.10E-06
response to external stimulus	1.60E-05
response to pest/pathogen/parasite	1.00E-04
1-month-old	
steroid metabolism	1.80E-05
steroid biosynthesis	4.00E-05
lipid metabolism	7.10E-05
lipid biosynthesis	3.20E-04
C21-steroid hormone biosynthesis	5.10E-03

EASE score is the Fisher exact probability of obtaining the number of genes in a certain pathway in the list of differentially expressed genes by chance. EASE score was calculated by theme detection software EASE which can be downloaded from http://david.niaid.nih.gov.

Table 2

List of 68 early response genes identified both by GeneSpring group comparison and by GCOS individual pair comparison algorithms.

Affy ID	FC	Name	GeneBank	Description
94120_s_at	224	Sprr2f	AJ005564	small proline-rich protein 2F
104388_at	19.6	Ccl9	U49513	chemokine (C-C motif) ligand 9
160901_at	19.5	Fos; c-fos	V00727	c-fos oncogene.
104374_at	19.2	Serpina3n	M64086	serine (or cysteine) proteinase inhibitor, clade A, member 3N
93871_at	17.5	Il1rn; IL-1ra	L32838	germline interleukin 1 receptor antagonist (IL-1rn) gene
92232_at	13.4	Socs3	U88328	suppressor of cytokine signaling 3
102736_at	12.6	Ccl2; MCP1	M19681	platelet-derived growth factor-inducible protein (JE) gene
102048_at	11.5	Ankrd1	AF041847	ankyrin repeat domain 1 (cardiac muscle)
101753 _s_at	10.8	Lzp-s	X51547	P lysozyme structural
100325_at	10.3	Gp49b	M65027	glycoprotein 49 B
95338_s_at	10.2	Mmp12	M82831	matrix metalloproteinase 12
160564_at	10.2	Lcn2	X81627	24p3 gene.
102860_at	9.0	Serpina3g	M64085	serine (or cysteine) proteinase inhibitor, clade A, member 3G
93497_at	8.8	C3	K02782	complement component 3
100611_at	8.7	Lzm	M21050	precursor; Mouse lysozyme M gene, exon 4.
102255_at	8.6	Osmr	AB015978	oncostatin M receptor
162206_f_at	6.2	Socs3 est	AV374868	suppressor of cytokine signalling-3 (SOCS-3) mRNA,
102914_s_at	6.2	Bcl2a1b	U23778	hematopoietic-specific early-response A1-b protein (A1b) gene
103486_at	6.0	Il1b	M15131	interleukin 1 beta
92550_at	6.0	Krt1-19	M36120	keratin 19 gene, complete cds.
93869_s_at	5.4	Bcl2a1d	U23781	hematopoietic-specific early-response A1-d protein (A1d) gene
161294_f_at	5.3	Clu	AV003873	C57BL/6J kidney cDNA clone 0610037O09, mRNA sequence.
98088_at	5.0	Cd14	X13333	CD14 antigen
96704_at	4.8	Sfn	AF058798	stratifin
99927_at	4.5	Cfi	U47810	complement component factor i
98772_at	4.4	Cxcl5	U27267	chemokine (C-X-C motif) ligand 5
94939_at	4.3	Cd53	X97227	CD53 antigen
95286_at	4.3	Clu	D14077	clusterin
160923_at	3.6	Abp1	AI197481	EST with weak similarity to diamine oxidase
93435_at	3.5	Cyp24a1	D89669	cytochrome P450, family 24, subfamily a, polypeptide 1
161046_at	3.5	Crlf1	AA270365	cytokine receptor-like factor 1
104155_f_at	3.5	Atf3	U19118	activating transcription factor 3
98988_at	3.5	AA408868	AA614971	expressed sequence AA408868
96752_at	3.4	Icam1	M90551	intercellular adhesion molecule 1 (ICAM-1) gene
102362_i_at	3.3	Junb	U20735	transcription factor junB (junB) gene
92559_at	3.1	Vcam1	U12884	vascular cell adhesion molecule 1
101464_at	3.0	Timp1	V00755	tissue inhibitor of metalloproteinase 1
102121_f_at	3.0	Krt1-19 est	AU040563	four-cell-embryo cDNA

Affy ID	FC	Name	GeneBank	Description
103448_at	3.0	S100a8	M83218	S100 calcium binding protein A8 (calgranulin A)
99057_at	2.9	Thy1	M12379	Thy-1.2 glycoprotein; Mouse Thy-1.2 glycoprotein gene
93866_s_at	2.8	Mglap	D00613	matrix gamma-carboxyglutamate (gla) protein
101410_at	2.7	Cldn4	AB000713	claudin 4
92925_at	2.7	Cebpb	M61007	CCAAT/enhancer binding protein (C/EBP), beta